Evolution and Mixing in Low and Intermediate Mass Stars

John C. Lattanzio

Department of Mathematics, Monash University,
Clayton, Victoria, 3168, Australia;
and
Institute of Astronomy, Madingley Road, Cambridge, U.K.

Abstract. I present a qualitative picture of our understanding of mixing and evolution in intermediate mass stars, with particular attention to changes in surface composition. The emphasis is on the mechanisms operating rather than a quantitative estimate of their magnitude.

1. INTRODUCTION

In this paper I will present a simple summary of the main phases of evolution of low and intermediate mass stars (roughly, 1–9$M_\odot$ on the main sequence), with particular emphasis on nucleosynthesis and mixing, because this is what concerns us most at this conference. To begin I will discuss the pre-Asymptotic Giant Branch (AGB) evolution of typical $1M_\odot$ and $5M_\odot$ stars, introducing terminology and physics as necessary. In section 4 I shall describe the thermally-pulsing AGB phase, with the phenomenon of Hot Bottom Burning (HBB) left to section 5. I leave the observational situation to be summarised by others elsewhere in this volume.

2. SUMMARY OF EVOLUTION AT $\sim$1M$_\odot$

We make the usual assumption that a star reaches the zero-age main sequence with a homeogeneous chemical composition (for an alternative evolutionary scenario see (1)). Figure 1 shows a schematic HR diagram for this star. Core H-burning occurs radiatively, and the central temperature and density grow in response to the increasing molecular weight (points 1–3). At central H exhaustion (point 4) the H profile is as shown in inset (a) in Figure 1. The star now leaves the main sequence and crosses the Hertzsprung Gap (points 5–7), while the central He core becomes electron degenerate and the nuclear burning is established in a shell surrounding this core. Inset (b) shows the advance of the H-shell during this evolution. Simultaneously, the star is expanding and the outer layers become convective. As the star reaches the Hayashi limit ($\sim$ point 7), convection extends quite deeply inward (in mass) from the surface, and the star ascends the (first) giant branch. The convective envelope

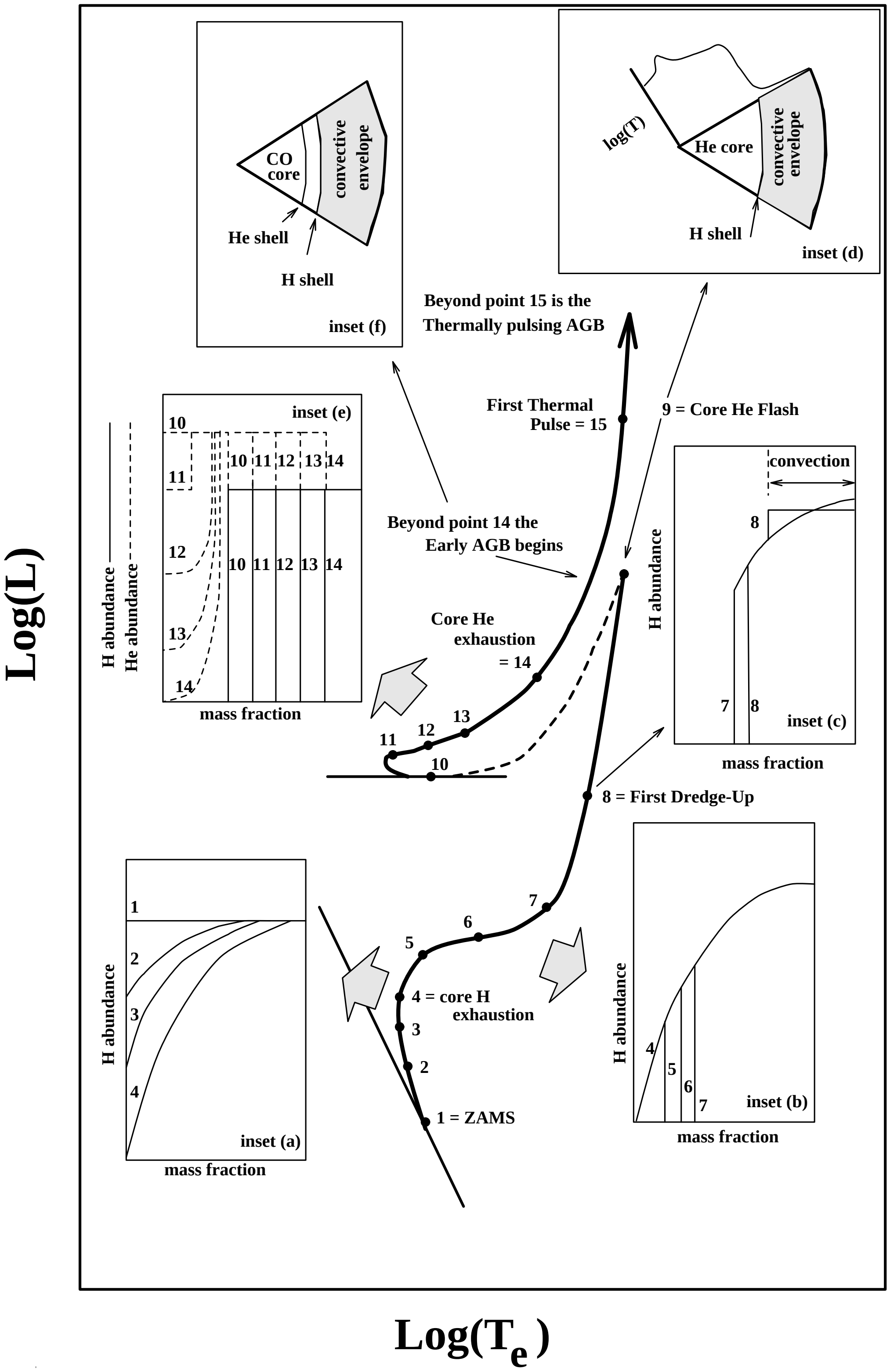

FIGURE 1. Schematic evolution at $\sim 1M_{\odot}$

penetrates into the region where partial H-burning has occured earlier in the evolution, as shown in inset (c) of Figure 1. This material is still mostly ^{1}H, but with added ^{4}He together with the products of CN cycling, primarily ^{14}N and ^{13}C. These are now mixed to the surface (point 8) and this phase is known as the "first dredge-up". The most important surface abundance changes are an increase in the ^{4}He mass fraction by about 0.03 (for masses less than about $4M_\odot$), while ^{14}N increases (at the expense of ^{12}C) by around 30%, and the number ratio ^{12}C/^{13}C varies between 18 and 26 (2).

As the star ascends the giant branch the He-core continues to contract and heat. Neutrino energy losses from the centre cause the temperature maximum to move outward, as shown in inset (d) of Figure 1. Eventually triple alpha reactions are ignited at this point of maximum temperature, but with a degenerate equation of state. The temperature and density are decoupled, and the resulting ignition is explosive, being referred to as the "core helium flash" (point 9: see for example (3)). Following this the star quickly moves to the Horizontal Branch where it burns ^{4}He gently in a convective core, and H in a shell (which provides most of the luminosity). This corresponds to points 10–13 in Figure 1. Helium burning increases the mass fraction of ^{12}C and ^{16}O (the latter through $^{12}\mathrm{C}(\alpha,\gamma)^{16}\mathrm{O}$) and the outer regions of the convective core become stable to the Schwarzschild convection criterion but unstable to that of Ledoux: a situation referred to as "semiconvection" (space prohibits a discussion of this phenomenon, but an excellent physical description is contained in (4 and 5)). Thus the composition profile in this region adjusts itself to produce convective neutrality, with the profiles as shown in inset (e) of Figure 1.

Following He exhaustion (point 14) the star ascends the giant branch for the second time, and this is known as the Asymptotic Giant Branch or AGB. The C-O core (the proportions of ^{12}C and ^{16}O depend on the uncertain rate for the $^{12}\mathrm{C}(\alpha,\gamma)^{16}\mathrm{O}$ reaction) becomes degenerate, and the star's energy output is provided by the He-burning shell (which lies immediately above the C-O core) and the H-burning shell. Above both is the deep convective envelope. This structure is shown in inset (f) in figure 1. We will later see that the He-shell is thermally unstable, as witnessed by the recurring "thermal pulses". Thus the AGB is divided into two regions: the early-AGB, prior to (and at lower luminosities than) the first thermal pulse, and the thermally-pulsing AGB beyond this. We will return to this in section 4.

3. SUMMARY OF EVOLUTION AT $\sim 5\mathrm{M}_\odot$

A more massive star, say of $\sim 5M_\odot$, begins its life very similarly to the lower mass star discussed above. The main initial difference is that the higher temperature in the core causes CNO cycling to be the main source for H-burning, and the high temperature dependence of these reactions causes a convective core to develop. As H is then burned into He the opacity (due mainly to electron scattering, and hence proportional to the H content) de-

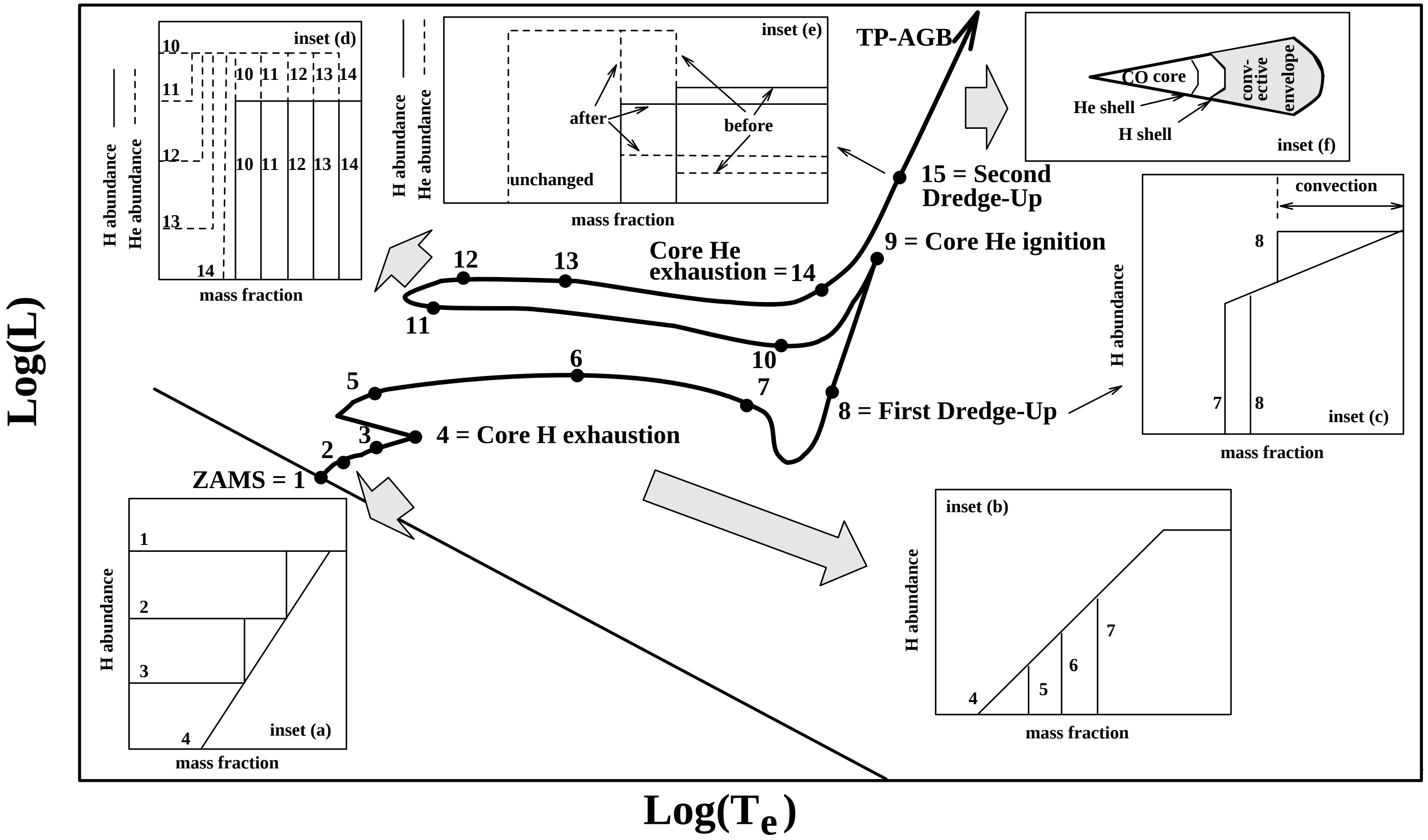

FIGURE 2. Schematic evolution at $\sim 5M_{\odot}$.

creases and the extent of the convective core decreases with time. This corresponds to points 1–4 in Figure 2. Following core H exhaustion there is a phase of shell burning as the star crosses the Hertzsprung Gap (points 5–7 and inset (b)), and then ascends the (first) giant branch. Again the inward penetration of the convective envelope (point 8) reaches regions where there has been partial H-burning earlier in the evolution, and thus these products (primarily ^{13}C and ^{14}N, produced at the cost of ^{12}C) are mixed to the surface in the first dredge-up, just as seen at lower masses, and sketched in inset (c) of figure 2.

For these more massive stars the ignition of ^{4}He occurs in the centre and under non-degenerate conditions, and the star settles down to a period of quiescent He-burning in a convective core, together with H-burning in a shell (see inset (d) in figure 2). The competition between these two energy sources determines the occurrence and extent of the subsequent blueward excursion in the HR diagram (e.g. (6)), when the star crosses the instability strip and is observed as a Cepheid variable (points 10–14). Following core He exhaustion the structural re-adjustment to shell He burning results in a strong expansion, and the H-shell is extinguished as the star begins its ascent of the AGB. With this entropy barrier removed, the inner edge of the convective envelope is free to penetrate the erstwhile H-shell. Thus the products of complete H-burning are mixed to the surface in what is called the "second dredge-up" (point 15). This again alters the surface compositions of ^{4}He, ^{12}C, ^{13}C and ^{14}N. This actually reduces the mass of the H-exhausted core, because in the process of mixing ^{4}He outward, of course, we also mix H inward (see inset (e) in figure 2). Note that there is a critical mass (of about $4M_{\odot}$, but dependent on composition) below which the second dredge-up does not occur. Following this the H-shell is re-ignited and the first thermal pulse occurs soon after: the star has reached the TP-AGB. Note that at this stage the structure is qualitatively similar for all masses.

4. THE THERMALLY-PULSING AGB

This has been reviewed in detail in many places (7, 8, 9, 10) and here we give only a brief summary. The He-burning shell is thermally unstable and experiences periodic outbursts called "shell flashes" or "thermal pulses". The four phases of such a thermal pulse are shown schematically in Figure 3. These are: (a) the off phase, where the structure is basically that of a pre-TP-AGB star. During this phase almost all of the surface lumosity is provided by the H-shell. This phase lasts for 10^4 to 10^5 years, depending on the core-mass; (b) the "on" phase, when the He-shell burns very strongly, producing luminosities up to $\sim 10^8 L_{\odot}$. The energy deposited by these He-burning reactions is too much for radiation to carry, and a convective shell develops, which extends from the He-shell almost to the H-shell. This convective zone comprises mostly He (about 75%) and ^{12}C (about 22%), and lasts for about 200 years; (c) the "power down" phase, where the He shell begins to die down, and the

FIGURE 3. The four phases of a thermal pulse cycle.

convection is shut-off. The previously released energy drives a substantial expansion, pushing the H-shell to such low temperatures and densities that it is extinguished; (d) the "dredge-up" phase, where the convective envelope, in response to the cooling of the outer layers, extends inward and, in later pulses, beyond the H/He discontinuity (which previously was the H-shell) and can even penetrate the flash-driven convective zone. This results in the ^{12}C

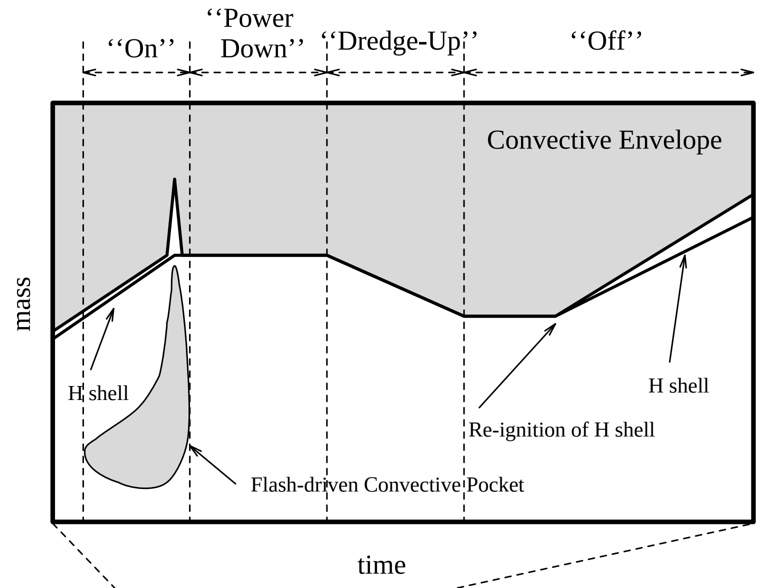

FIGURE 4 (a). One thermal pulse.

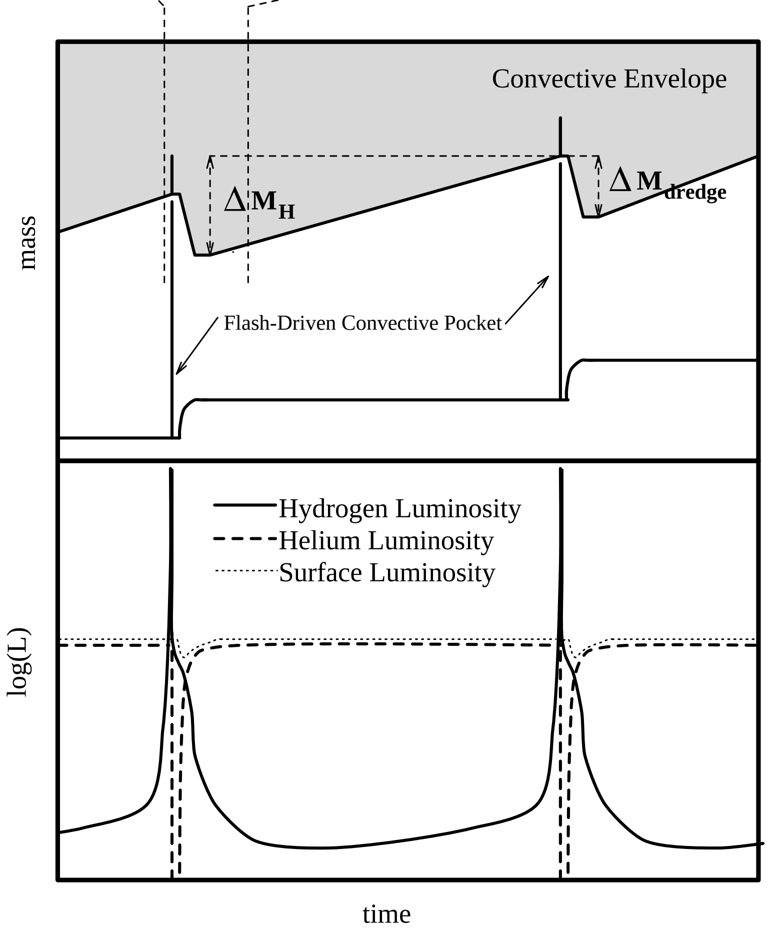

FIGURE 4 (b). Two consecutive thermal pulses which was produced by the He-shell, and mixed outward by the convective shell, now being mixed to the surface by the envelope convection. This is the "third dredge-up", and it qualitatively (and almost quantitatively) accounts for the occurrence of carbon stars at higher luminosities on the AGB (11, 12). Figure 4 shows these four phases during one pulse (top) and during two consecutive pulses (bottom). Also shown in the bottom panel is the variation of the total radiated luminosity and the two nuclear energy sources (i.e. the luminosities from H and He burning) during a pulse cycle.

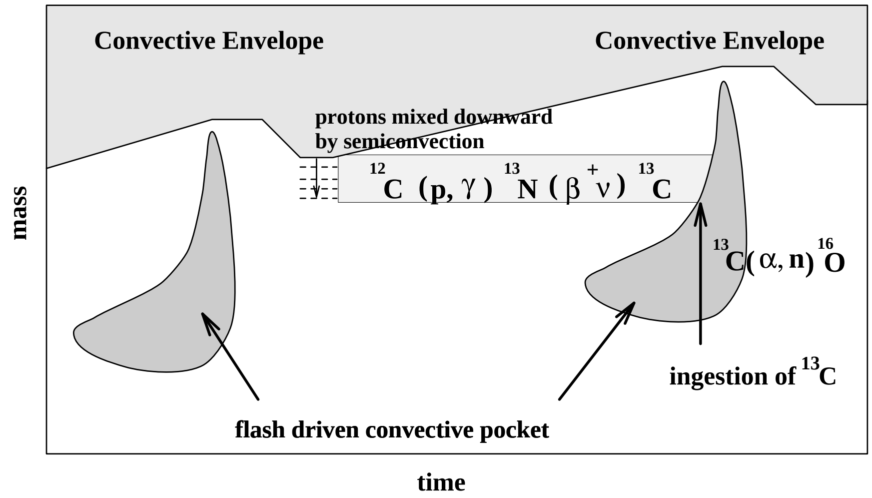

FIGURE 5. Schematic of ^{13}C neutron source.

It is now well established observationally that these stars also produce s-process elements (10, 13). It is also well established that ^{22}Ne is probably not the neutron source, but that a much more likely candidate is ^{13}C (14, 15). The basic result here is that following a pulse the bottom of the convective envelope can become semiconvective which will diffuse some protons downward beyond the formal maximum inward extent of the convective envelope during the third dredge-up phase. This is shown schematically in Figure 5. The protons which are deposited by this semiconvection are in a region comprising about 75% ^{4}He and 22% ^{12}C, so when the H-shell is re-ignited these protons are burned into ^{13}C (and ^{14}N). The scenario as usually envisaged is that when the next thermal pulse occurs this ^{13}C is engulfed by the flash-driven convection, and then in this ^{4}He-rich environment neutrons are released by $^{13}C(\alpha,n)^{16}O$. These neutrons are then captured by ^{56}Fe and its progeny to produce the observed s-process elements.

This scenario has many attractive features, but it also has some problems (8). In particular, one usually ignores the energy released by the $^{13}C(\alpha,n)^{16}O$ reactions, although this can be substantial, depending on the exact time of ingestion (16, 17). Perhaps a more serious concern is the discovery by Straniero

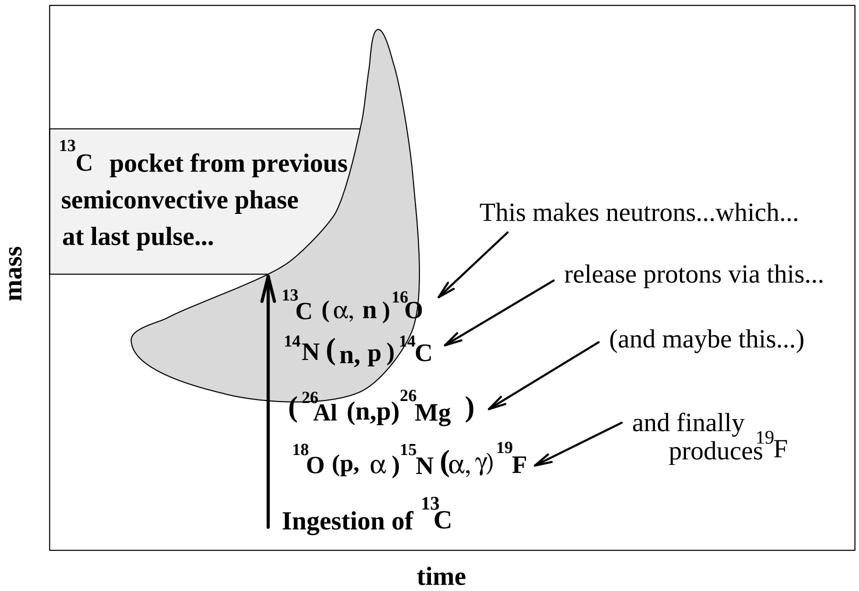

FIGURE 6. Schematic of probable ^{19}F production mechanism.

et al (18) that any ^{13}C formed during re-ignition of the H-shell is burned *radiatively* during the interpulse phase, so that there is no ^{13}C to be ingested at the next pulse! Thus the neutrons are produced, and the *s*-processing occurs, in a radiative zone. The consequences of this discovery are yet to be examined.

The recent discovery that the ^{19}F/^{16}O ratio in AGB stars increases with the ^{12}C/^{16}O ratio (19) implicates thermal pulses in the origin of this ^{19}F. The only paper to address this situation from the theoretical view is that of Forestini et al (20). They investigated many possible formation scenarios, and the one they judge as most favourable is illustrated in Figure 6. Here, some ^{13}C produces neutrons via the ^{13}C(α,n)^{16}O reaction discussed above. But some of these neutrons are captured by ^{14}N to produce ^{14}C and protons. These protons, plus possibly some from ^{26}Al(n,p)^{26}Mg, are then captured by ^{18}O and the sequence ^{18}O(p, α)^{15}N(α, γ)^{19}F then produces the observed ^{19}F, which is then dredged to the surface in the usual way, following the pulse. For all except those stars with the highest abundances of ^{19}F it appears that the amount of ^{13}C left from the CN cycling H-shell is sufficient. Nevertheless, some extra source of ^{13}C may be required. At present, however, the models overproduce ^{18}O. It remains to be seen if this problem can be overcome, but it may be tied closely to HBB (see below).

5. HOT BOTTOM BURNING

When Wood, Bessell and Fox (21) found bright AGB stars (possessing enhanced abundances of *s*-process elements) in the Magellanic Clouds it came as some surprise that these were not carbon stars, given the scenario outlined above. These authors speculated that these stars were undergoing HBB, where the temperature at the bottom of the convective envelope is sufficiently high that CN cycling can occur. Thus, some (or perhaps all, or even *more* than all !) of the ^{12}C that is added to the envelope via third dredge-up is then processed into ^{14}N, and the star may never become a carbon star. Subsequent observations by Smith and Lambert (22) showed that these stars possessed extremely strong lithium lines. This was interpreted as further evidence for HBB, as ^{7}Li is believed to be produced by the "beryllium transport mechanism" of Cameron and Fowler (23). Here we require fairly high temperatures to begin the cycle with α-captures on ^{3}He to produce ^{7}Be, as illustrated in the top panel of Figure 7. If this ^{7}Be is to remain at high temperatures, then we would find the PPIII cycle going to completion. Rather, we want the ^{7}Be to β-decay to ^{7}Li. Likewise, this ^{7}Li could capture a proton, thus completing the PPII chain, which we do not want either. We see that the mechanism requires production of ^{7}Be and then transport of that ^{7}Be to cooler regions, as would be expected in a convective envelope. That such a scenario works quantitatively was demonstrated by Boothroyd and Sackmann (24). The lower panel in Figure 7 shows some calculations performed by Cannon et al (25). In this calculation we calculate separately the composition of the upward moving (dashed lines) and downward moving (solid lines) flows. Thus we see clearly the production of ^{7}Be at the bottom of the convective envelope, as well as the reduced abundance of ^{7}Be in the downflows. This is because in the outer envelope much of the ^{7}Be has decayed into ^{7}Li, which is also seen in the enhanced ^{7}Li composition in the downflows (note that the scale is logarithmic). Hence the mechanism works exactly as envisaged. Of course, the duration of the super-lithium-rich phase is limited, for the ^{7}Li produced is mixed through the hot bottomed envelope on each convective cycle, and thus some ^{7}Li is destroyed on each passage. Further, the amount of ^{3}He available for synthesis into ^{7}Li is also limited, and once it is used it is gone. For further details, and a quantitative analysis, see Boothroyd and Sackmann (24).

It was shown by Blöcker and Schönberner (26) that stars undergoing HBB (roughly, those with masses greater than about $5M_{\odot}$) do not follow the core-mass–luminosity relation (see also (27) and (28)). Further, convective envelopes have been found to reach nearly to 100 million K during the interpulse phase. This is certainly hot enough for the Ne-Na and Mg-Al cycles to operate. No quantitative studies of this phase have been performed to date (but see 25 for some preliminary studies). Such calculations hold the promise of explaining some of the aluminium enhancements seen in SiC and oxide grains (see papers on meteoritic analysis elsewhere in this volume). Indeed, Boothroyd, Sackmann and Wasserburg (29) have applied these models to a quantitative understanding of the oxygen isotopic ratios in meteorites. (See this paper, also, for a discussion of the changes in oxygen isotoic ratios which result from the first and second dredge-up episodes.)

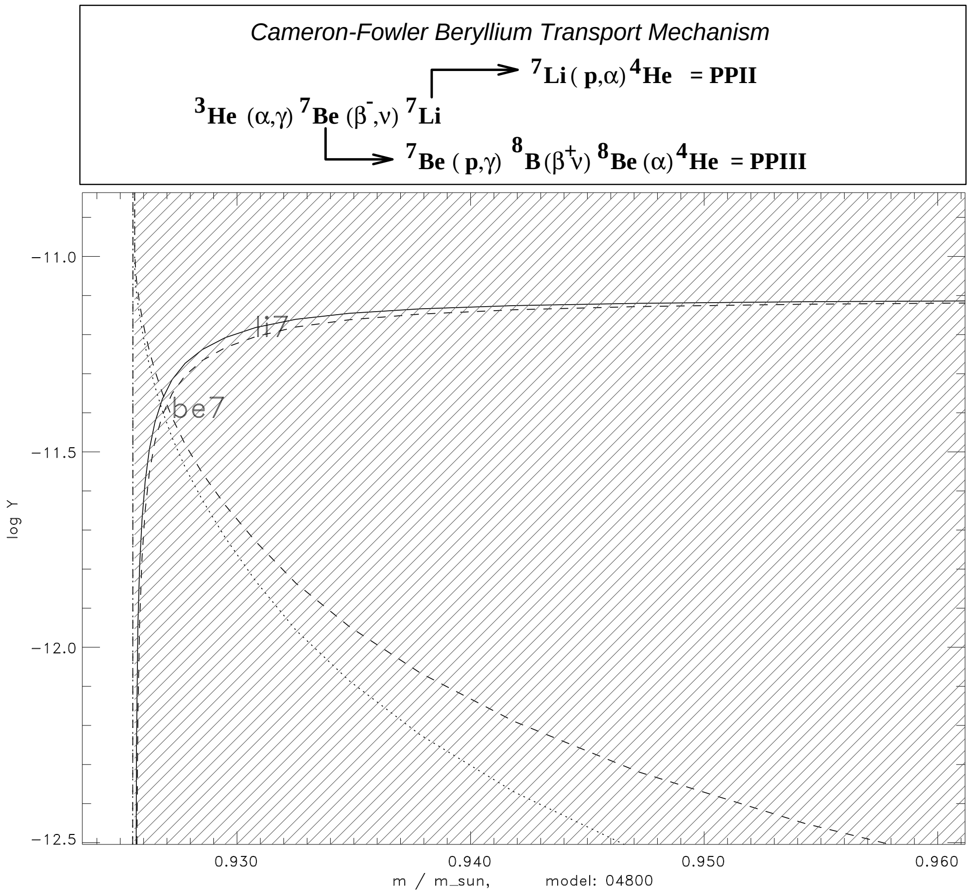

FIGURE 7. Lithium production by HBB in the $5M_{\odot}$ model of Cannon et al (25). The cross-hatched region denotes convection.

6. CONCLUSIONS

In this paper I have tried to give a qualitative summary of the different nuclear paths and mixing events which occur in the lives of low and intermediate mass stars (roughly, 1–9 $M_{\odot}$). Although this is an extremely short phase of a star's life (under 10^6 years) the TP-AGB is important for many reasons. It exhibits complex nucleosynthesis (I have barely touched on the subject of s-processing !) combined with normal convective mixing and semi-convection. One must add to this the possibility of overshoot. Hence an understanding of these stars could help us to understand much of the physics operating in their interior. Further, the strong stellar winds which accompany this phase are responsible for depositing the products of the nucleosynthesis into the interstellar medium, where they form the material from which the next stellar generation will form. We are now on the verge of a new quantitative understanding of these processes because of the close interation between theory and observation, including recent meteoritic analysis. The future looks very exciting indeed !

REFERENCES

1. Lattanzio, J. C., *MNRAS*, **207**, 309 (1984).
2. Charbonnel, C., *A. & A.*, **282**, 811 (1994).
3. Deupree, R. G., *Ap. J.*, **287**, 268 (1984).
4. Castellani, V., Giannone, P., and Renzini, A., *Astr. Sp. Sci*, **10**, 340 (1971).
5. Castellani, V., Giannone, P., and Renzini, A., *Astr. Sp. Sci*, **10**, 355 (1971).
6. Lauterborn, D., Refsdal, S., and Weigert, A., *A. & A.*, **10**, 97 (1971).
7. Iben, I., Jr., and Renzini, A., *A. R. A. & A.*, 21, 271 (1983).
8. Lattanzio, J. C., "Evolution and Mixing on the AGB" in *Evolution of Peculiar Red Giants*, 1989, p 161.
9. Sackmann, I.-J., and Boothroyd, A., "On Low Mass AGB Stars" in *Evolution of Stars: The Photospheric Abundance Connection"*, 1991, p 275.
10. Iben, I., Jr., "Asymptotic Giant Branch Stars: Thermal Pulses, Carbon Production, and Dredge-Up; Neutron Sources and *s*-process Nucleosynthesis", in *Evolution of Stars: The Photospheric Abundance Connection"*, 1991, p 257.
11. Groenewegen, M. A. T., and de Jong, T., *A. & A.*, **267**, 410 (1994).
12. Lattanzio, J. C., *Ap. J.*, **313**, L15 (1987).
13. Lambert, D. L., "The Chemical Composition of Asymptotic Giant Branch Stars–The *s*-Process", in *Evolution of Stars: The Photospheric Abundance Connection"*, 299 (1991).
14. Iben, I., Jr., and Renzini, A., *Ap. J. Lett.*, **259**, L79 (1982).
15. Iben, I., Jr., and Renzini, A., *Ap. J. Lett.*, **263**, L23 (1982).
16. Bazan, G., and Lattanzio, J. C., *Ap. J.*, **409**, 762 (1993).
17. Mowlavi, N., et al., this volume.
18. Straniero, O., et al., this volume.
19. Jorissen, A., Smith, V. V.,and Lambert, D., L., *A. & A.*, **261**, 164 (1992).
20. Forestini, M., Goriely, S., Jorissen, A., and Arnould, M., *A. & A.*, **261**, 157 (1992).
21. Wood, P. R., Bessell, M. S., and Fox, M. W., *Ap. J.*, **272**, 99 (1983).
22. Smith, V. V., and Lambert, D. L., *Ap. J.*, **345**, L75 (1989).
23. Cameron, A. G. W., and Fowler, W. A., *Ap. J.*, **164**, 111 (1971).
24. Boothroyd, A. I., and Sackmann, I.-J., *Ap. J. Lett.*, **392**, L71 (1992).
25. Cannon, R. C., et al., this volume.
26. Blöcker, T., and Schönberner, D., *A. & A.*, **244**, L43 (1991).
27. Lattanzio, J. C., *Proc. Astron. Soc. Aust.*, **10**, 120 (1992).
28. Boothroyd, A. I., and Sackmann, I.-J., *Ap. J. Lett.*, **393**, L21 (1993).
29. Boothroyd, A. I., Sackmann, I.-J., and Wasserburg, G. J., preprint.